scientific reports

Check for updates

OPEN

Predictive value of subharmonic-aided pressure estimation for diagnosing clinically significant portal hypertension

Yoshiko Nakamura[1], Masashi Hirooka[1]✉, Ryo Yano[1], Naohisa Kamiyama[2], Takuma Oguri[2], Toyoki Shimamoto[1], Makoto Morita[1], Yuki Okazaki[1], Atsushi Yukimoto[1], Naoki Fukuyama[3], Takao Watanabe[1], Teruki Miyake[1], Osamu Yoshida[1], Yoshio Tokumoto[1], Masanori Abe[1] & Yoichi Hiasa[1]

Subharmonic-aided pressure estimation (SHAPE) is an innovative ultrasound-based method using contrast agents to assess the severity of portal hypertension (PH). This study aimed to evaluate the predictive value of the revised SHAPE method for diagnosing clinically significant PH (CSPH; hepatic venous pressure gradient [HVPG] ≥ 10 mmHg). This cross-sectional study included 62 patients with chronic liver disease who underwent HVPG, liver stiffness, and spleen stiffness (SSM) measurements. Cutoff values for high sensitivity and specificity were derived to rule in CSPH. The SHAPE gradient showed a strong correlation with HVPG (r = 0.74, $p < 0.01$). Patients with CSPH had a significantly higher SHAPE gradient than those without CSPH (− 1.6 dB versus − 5.1 dB; $p < 0.01$). The optimal cutoff value was − 2.7 dB; the sensitivity, specificity, and positive and negative predictive values were 92%, 87%, 81%, and 94%, respectively. The AUC value for predicting CSPH was 0.94 for the SHAPE method, compared with 0.76 for Baveno VII, 0.78 for the Baveno VII-SSM dual method, and 0.81 for the single-cutoff algorithm. The revised SHAPE method is a highly accurate, non-invasive tool for assessing HVPG and predicting CSPH in clinical practice, offering a potential alternative to current invasive measures.

Keywords Subharmonic-aided pressure, Portal hypertension, Liver cirrhosis, Baveno VII criteria, Liver cirrhosis, Liver stiffness measurement

Portal hypertension (PH) is a critical pathophysiological feature of cirrhosis that causes complications and increases the mortality rate[1]. Hepatic venous pressure gradient (HVPG) measurement is the gold standard for assessing and staging PH[2,3], with an HVPG > 5 mmHg indicating sinusoidal PH and an HVPG ≥ 10 mmHg defining clinically significant PH (CSPH)[4,5]. Historically, management of PH has focused on the prevention of variceal bleeding. However, treatment strategies have shifted toward early intervention to prevent decompensation[5,6]. Despite its clinical significance, the invasive nature and limited accessibility of HVPG measurement restrict its routine application, highlighting the need for reliable and readily available non-invasive tests (NITs)[7].

Advanced chronic liver disease has emerged as a framework for NIT-based evaluation that incorporates blood- and imaging-based assessments. The liver stiffness measurement (LSM) combined with the platelet count (PLT) has been validated as a surrogate marker and widely applied. The Baveno VII consensus guidelines recommend these markers for the diagnosis of CSPH[5]. However, a considerable proportion of patients remain in the indeterminate zone, highlighting the need for refinement. The spleen stiffness measurement (SSM), which directly reflects intrasplenic congestion and pressure, has emerged as a promising surrogate method for assessing PH[8]. The Baveno VII consensus recognizes its potential but notes challenges such as higher failure rates and technical limitations of existing SSM probes, which hinder broader clinical adoption.

Ultrasound contrast agents (UCAs), composed of gas-filled microbubbles, exhibit unique nonlinear scattering properties when immersed at pressures above 200 kPa[9]. This scattering spans a wide frequency spectrum, allowing for contrast-specific imaging modes. In particular, subharmonic imaging (SHI) leverages

[1]Department of Gastroenterology and Metabology, Ehime University Graduate School of Medicine, 454 Toon, Ehime 791-0295, Japan. [2]Ultrasound General Imaging, GE HealthCare Japan, Hino-Shi, Japan. [3]Department of Radiology, Ehime University Graduate School of Medicine, Toon, Ehime, Japan. ✉email: hirooka.masashi.mb@ehime-u.ac.jp

these properties by transmitting at double the resonance frequency and receiving half the microbubble resonance frequency, thereby achieving UCA-specific signals with near-complete tissue suppression[10–12].

Subharmonic-aided pressure estimation (SHAPE), a new non-invasive pressure measurement technique, has recently become commercially available[13,14]. The subharmonic amplitude responses follow an S-curve pattern across varying acoustic pressures, with the growth stage showing a high sensitivity to hydrostatic pressure[15]. Although studies have demonstrated the utility of SHI for evaluating PH[16–18], particularly with power optimization algorithms, data on its accuracy remain limited. However, Kuroda et al. recently revised the approach to meet its clinical feasibility by integrating a single bolus injection and standardizing contrast-enhanced ultrasonography protocols[14]. These recent technical advances have introduced refinements aimed at enhancing its applicability and measurement accuracy. Thus, this study aimed to evaluate the predictive value of the revised SHAPE method in diagnosing CSPH, comparing its performance with established diagnostic approaches, and assessing its potential as a reliable non-invasive clinical tool.

Methods

Ethics statements, patients, and study design

This retrospective study was conducted in compliance with the Declaration of Helsinki and approved by the Institutional Ethics Committee of Ehime University Hospital (approval number: 2410005). The requirement for informed consent was waived because of the retrospective nature of the study. Due to the retrospective nature of the study, the Institutional Ethics Committee of Ehime University Hospital (approval number: 2410005) waived the need for obtaining informed consent.

Patients with chronic liver disease who underwent SHAPE for PH between February 2024 and August 2024 were consecutively included. In addition, this study consecutively enrolled patients without applying pre-specified thresholds such as LSM, FIB-4, or SSM, thereby minimizing the risk of selection bias related to prior non-invasive test results (Fig. 1). The inclusion criteria were the ability to follow breathing control instructions and the availability of HVPG measurements. The exclusion criteria were as follows: (1) hepatocellular carcinoma with portal vein (PV) or hepatic vein (HV) thrombosis, (2) absence of chronic liver injury, (3) poor image quality, (4) severe hepatic decompensation symptoms (i.e., overt hepatic encephalopathy, refractory ascites with infection, and portal hypertensive bleeding), (5) invalid LSM, and (6) incomplete blood test data.

Study endpoints

The primary endpoint was the correlation between the HVPG and SHAPE gradients. The secondary endpoint was the diagnostic performance of the SHAPE gradient for CSPH compared with the Baveno VII criteria and Baveno VII-SSM models[5,8].

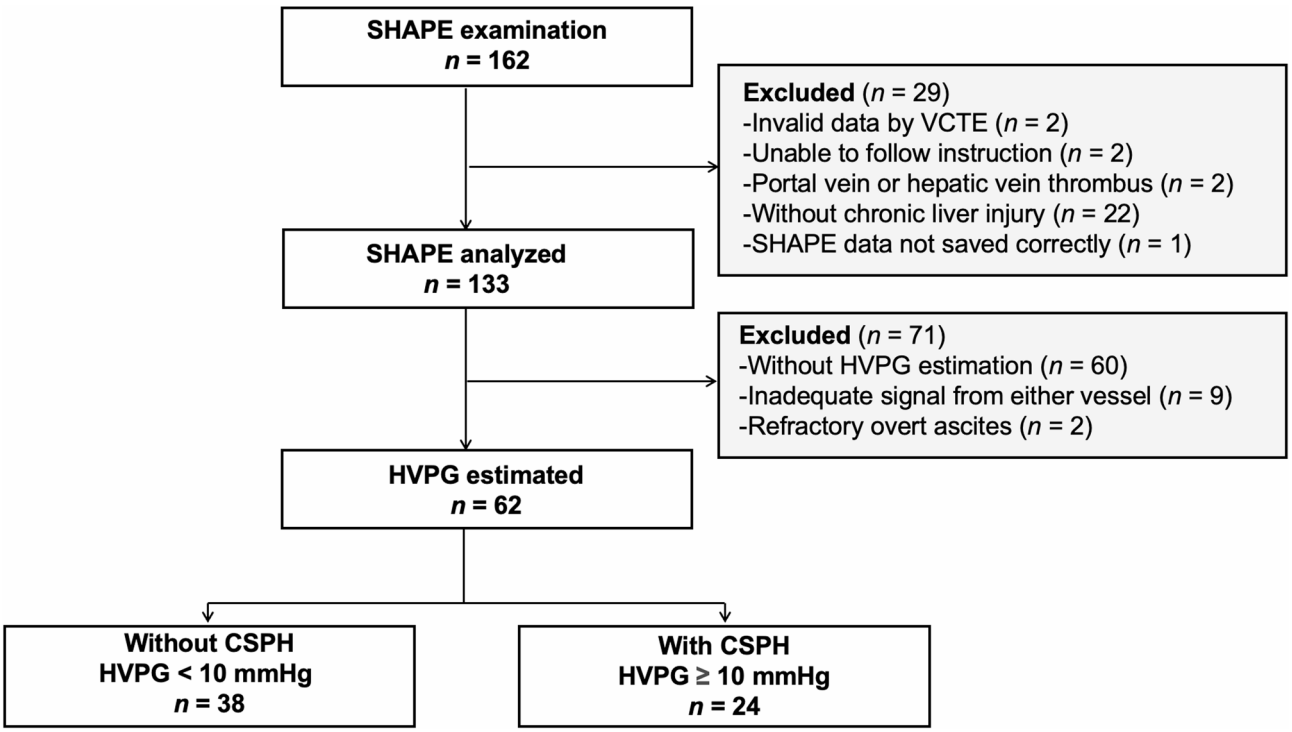

Fig. 1. Flowchart showing the patient enrollment process in this study. CSPH, clinically significant portal hypertension; VCTE, vibration-controlled transient elastography.

SHAPE examination

SHAPE examinations were performed under fasting conditions by two experienced sonographers (M.H. and Y.N., with 25 and 15 years of experience, respectively) using a Logiq E10 US scanner (GE HealthCare, Wauwatosa, WI, USA) subharmonic imaging software (research option). The ultrasound probe used was a C1-6-D convex prove with a center frequency of 3.5 MHz. The HV and PV were visualized at the same depth using the right intercostal approach. Perfluorobutane microbubbles (Sonazoid®; GE HealthCare, Amersham, UK), chosen for their superior pressure sensitivity[13], were administered intravenously at 0.06 μL/kg. Cine recordings commenced 90 s post-injection, capturing 20-s sequences during breath-hold, with the mechanical index incrementally increased by 0.05 every 0.5 s (Fig. 2a)[19].

Time-intensity curve analysis was performed using integrated software, with 10-mm diameter regions of interest set at equal depths in the PV and HV. Subharmonic amplitude-acoustic power relationships were derived, and the optimal acoustic power was determined as the maximum slope of the PV response curve[12]. The SHAPE gradient was calculated as the difference between the HV and PV subharmonic signals (HV-PV) at this optimal power (Fig. 2b, c).

SHAPE examinations were performed between February 2024 and August 2024, with all cine loops preserved in Digital Imaging and Communications in Medicine (DICOM) format. These stored data were subsequently re-analyzed according to the revised SHAPE methodology[14]. The analytic protocol of the SHAPE method used in this study was available to us through direct communication with the authors prior to its formal publication, and the same procedures were subsequently published by Kuroda et al.[14] Thus, our analysis strictly followed the validated methodology despite the later publication date.

HVPG measurement

The HVPG was measured within 1 week of the SHAPE examination using a 5-French balloon-tipped catheter. The right HV was catheterized via the right femoral vein or right internal jugular vein. The HVPG was calculated as the difference between the wedged and free hepatic venous pressures.

LSM and SSM

LSM and SSM were performed using vibration-controlled transient elastography (FibroScan 502; Echosens, Paris, France) with an M-probe and were validated by two hepatologists. The medians of 10 valid measurements (kPa) were recorded. Measurements with an interquartile range (IQR)/median ratio ≥ 30% were deemed unreliable. For the SSM-based models, patients with failed SSM owing to inadequate spleen size or volume were classified on the basis of LSM and PLT.

Diagnostic algorithms for CSPH

CSPH was defined as an HVPG ≥ 10 mmHg. The following algorithms were applied:

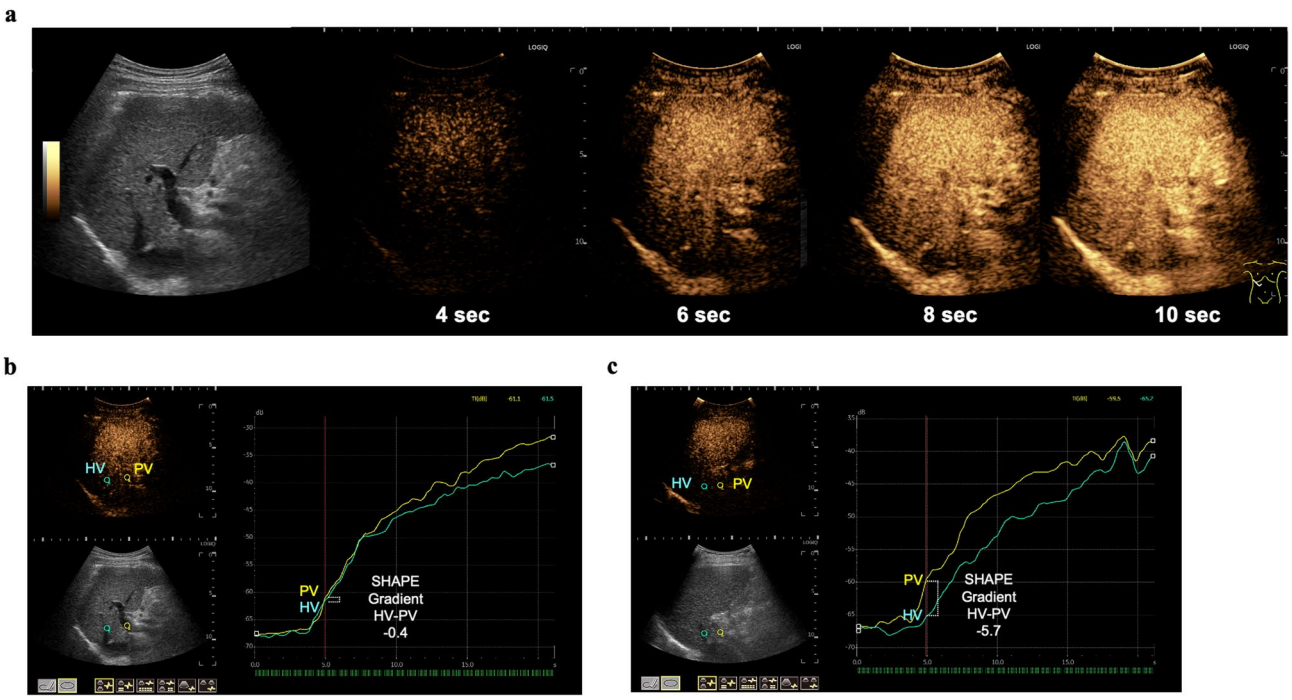

Fig. 2. Representative images (**a**) B-mode and temporal subharmonic contrast images during the increase of the mechanical index. (**b**, **c**) Representative examples of time intensity curve analysis. The SHAPE gradient (HV-PV) values are (**b**) − 0.4 dB with a HVPG of 12 mmHg and (**c**) − 5.7 dB with a HVPG of 4 mmHg. HV, hepatic vein; PV, portal vein; SHAPE, subharmonic-aided pressure estimation.

Baveno VII criteria[5]**:** CSPH was ruled out if the LSM was ≤ 15 kPa and PLT was ≥ 150 G/L; CSPH was ruled in if LSM was ≥ 25 kPa.
Baveno VII-SSM single-cutoff model[8]**:** CSPH was ruled out if at least two of the following criteria were met: LSM ≤ 15 kPa, PLT ≥ 150 G/L, and/or SSM ≤ 40 kPa. However, CSPH was ruled in if at least two of the following criteria were met: LSM ≥ 25 kPa, PLT < 150 G/L, and/or SSM > 40 kPa.
Baveno VII-SSM dual-cutoff model[8]**:** This was similar to the single-cutoff model except for the SSM thresholds of < 21 kPa for ruling out CSPH and > 50 kPa for ruling in CSPH.

Patients who did not meet the rule-in or rule-out criteria were designated as "gray zone".

Statistical analysis

Continuous variables are expressed as medians with interquartile ranges (IQRs; 25th–75th percentiles), and categorical variables are presented as percentages. Between-group comparisons were performed using the Wilcoxon rank-sum test for continuous variables and the chi-square or Fisher exact tests for categorical variables. The inter-rater reliability of the SHAPE measurements was assessed using the Bland–Altman analysis, including 95% limits of agreement and evaluation of fixed and proportional errors. Intraclass correlation coefficients (ICCs) were used to assess reliability, with ICC > 0.80 indicating excellent agreement.

Relationships between variables were analyzed using Spearman correlation coefficients. The required sample size was 25 individuals based on a correlation coefficient of $\rho = 0.5$, significance level of $\alpha = 0.05$, and statistical power $(1 - \beta)$ of 0.8. Given the retrospective nature of this study, we aimed to analyze more than 25 cases. The diagnostic performance for CSPH prediction was evaluated using receiver operating characteristic (ROC) curve analysis, calculating the area under the ROC curve (AUC), sensitivity, specificity, positive predictive value (PPV), and negative predictive value (NPV). The optimal SHAPE threshold was determined using the Youden index. Statistical significance was defined as $p < 0.05$, and analyses were performed using STATA (version 15.0; StataCorp, College Station, TX, USA).

Results

Patient characteristics

The final analysis included 62 patients (Fig. 1), and the study population consisted of 44 men (70%), with a median SHAPE gradient of − 3.7 dB. Underlying liver diseases included viral hepatitis (n = 31, 50%), metabolic dysfunction-associated steatotic liver disease (n = 15, 24%), alcohol-associated liver disease (n = 13, 22%), and other diseases (n = 5, 4%). The median HVPG was 7.5 mmHg, and the distribution is shown in the supplementary Fig. S1. Detailed patient characteristics are presented in Table 1.

Agreement of the SHAPE measurement

Interobserver analysis of the SHAPE measurements between the two hepatologists demonstrated excellent absolute agreement (ICC 0.95 [95% confidence interval {CI} 0.89–0.97]). The reproducibility between the two observers was assessed using Bland–Altman analysis, which revealed a fixed bias of 0.347 (95% CI 0.034–0.660). The Pitman test showed no significant differences between the observers ($p = 0.299$, r = 0.178) (Supplementary Fig. S2).

Correlation between HVPG and the SHAPE gradient

The SHAPE gradient exhibited a strong linear correlation with HVPG across all measurements (r = 0.74, $p < 0.01$) (Fig. 3a). Additionally, significant correlations were observed between the HVPG and other parameters, including LSM (r = 0.75), SSM (r = 0.51), Model for End-Stage Liver Disease (MELD) score (r = 0.25), and Fibrosis-4 (FIB-4) index (r = 0.43).

Diagnostic performance of the SHAPE gradient

Patients were divided into two groups based on their HVPG values: those without CSPH (n = 38) and those with CSPH (n = 24) (Table 1). The CSPH group showed significantly higher MELD scores, albumin-bilirubin scores, FIB-4 index values, LSM, SSM, and laboratory fibrosis markers (hyaluronic acid and type IV collagen). High-risk esophagogastric varices were more common in the CSPH group than in the non-CSPH group (25% [n = 6] versus 5% [n = 2]; $p = 0.04$).

The SHAPE gradient was significantly higher in patients with CSPH (− 1.6 dB [− 2.3, 0.2]) than in those without CSPH (− 5.1 dB [− 6.4, − 3.9]; $p < 0.01$) (Table 1, Fig. 3b). For CSPH prediction, the SHAPE gradient achieved an AUC of 0.94 (95% CI 0.88–1.0) (Fig. 4). The optimal cutoff value of − 2.7 dB, determined using the Youden index, demonstrated a sensitivity, specificity, PPV, and NPV of 92%, 87%, 81%, and 94%, respectively.

Comparative analysis of CSPH diagnostic methods

The proportion of patients who had inadequate SSM measurements was 22% (n = 14). Patients were classified according to the three diagnostic algorithms (Table 2). The proportions of patients in the unclassified zone were 44% (n = 27) for the Baveno VII model, 27% (n = 17) for the Baveno VII-SSM dual-cutoff model, and 15% (n = 9) for the Baveno VII-SSM single-cutoff model.

Diagnostic performance metrics revealed that the Baveno VII criteria achieved a PPV of 93% and a NPV of 95% (AUC: 0.76), whereas the Baveno VII-SSM dual-cutoff model showed a PPV of 84% and a NPV of 96% (AUC: 0.78). The Baveno VII-SSM single-cutoff model demonstrated a PPV of 82% and a NPV of 94% (AUC: 0.81).

Variable	All patients ($n=62$)	Patients without CSPH ($n=38$)	Patients with CSPH ($n=24$)	p value
HVPG (mmHg)	7.5 (5, 12)	5 (4, 7)	14 (11, 16)	< 0.01
Age (years)	75 (68, 80)	75 (69, 82)	73.5 (68, 76)	0.25
Male sex (%)	44 (70)	28 (74)	16 (67)	0.58
Body mass index (kg/m^2)	24.7 (22.4, 27.5)	24.8 (22.0, 27.1)	24.5 (22.5, 28.8)	0.39
Etiology;	31/15/13/3	22/8/7/1	9/7/6/2	0.53
Virus/MASLD/ALD/Other diseases				
High-risk varices (%)	8 (13)	2 (5)	6 (25)	0.04
MELD score	3 (1, 7)	2.5 (1, 6)	4.5 (2.5, 9.5)	0.04
MELD-Na score	3.5 (0, 6)	1.5 (− 1, 6)	4.5 (1.5, 11.5)	0.03
Child–Pugh score; 5/6/7/8/9/10	41/9/6/4/2/0	30/5/2/1/0/0	11/4/4/3/2/0	0.03
ALBI score	− 2.63 (− 2.93, − 2.14)	− 2.77 (− 2.95, − 2.60)	− 2.26 (− 2.61, − 1.85)	< 0.01
FIB-4 index	4.33 (2.68, 5.71)	3.19 (1.96, 4.34)	5.54 (4.71, 8.55)	< 0.01
Laboratory parameter				
Albumin (g/dL)	4.0 (3.5, 4.3)	4.2 (3.9, 4.4)	3.6 (3.4, 3.9)	< 0.01
Total bilirubin (mg/dL)	1.0 (0.7, 1.2)	0.8 (0.6, 1.0)	1.1 (0.8, 1.5)	0.02
ALT (U/L)	22 (16, 35)	20 (15, 28)	33 (20, 47)	0.01
Platelet count (G/L)	13.1 (9.4, 18.9)	15.6 (11.5, 20.6)	10.6 (8.3, 13.8)	< 0.01
Prothrombin time (%)	85.7 (68.7, 100.1)	90.4 (76, 102.4)	80 (65, 92)	0.02
Ammonia (μg/dL)	47 (35, 72)	42 (33, 65)	56 (39, 96)	0.10
M2BPGi (COI)	2.04 (1.05, 4.04)	1.25 (0.92, 2.05)	4.08 (2.78, 7.37)	< 0.01
Hyaluronic acid (ng/mL)	134 (82, 321)	99 (53, 150)	308 (141, 481)	< 0.01
Collagen type IV (ng/mL)	5.8 (4.1, 8.9)	4.6 (4.0, 6.3)	8.9 (6.8, 12.0)	< 0.01
LSM by VCTE (kPa)	13.9 (7.2, 21.4)	9.7 (6.1, 13.8)	25.7 (18.6, 37.8)	< 0.01
SSM by VCTE (kPa)	30.3 (20.7, 52.7)	21.1 (17.4, 30.4)	52.3 (31.8, 67.9)	< 0.01
SHAPE gradient (dB)	− 3.7 (− 5.5, − 1.8)	− 5.1 (− 6.4, − 3.9)	− 1.6 (− 2.3, 0.2)	< 0.01

Table 1. Patient characteristics. Quantitative variables are presented as the median and interquartile range. *ALD* alcoholic liver disease; *ALT* aspartate aminotransferase; *ALBI* albumin-bilirubin; *FIB-4* fibrosis-4; *MASLD* metabolic dysfunction-associated liver disease; *MELD* model for end-stage liver disease; *M2BPGi* Mac-2 binding protein glycosylation isomer; *HVPG* hepatic venous pressure gradient; *LSM* liver stiffness measurement; *SHAPE* subharmonic-aided pressure estimation; *SSM* spleen stiffness measurement; *VCTE* vibration-controlled transient elastography.

Although the Baveno VII-SSM single-cutoff algorithm showed improved performance over the Baveno VII criteria alone, with fewer gray zone cases and a higher AUC, the SHAPE gradient exhibited superior accuracy in identifying patients with CSPH.

Additionally, patients with unclassified zone for the Baveno VII model were analyzed. The population of unclassified zone for Baveno VII model consisted of 15 men (56%), with a median HVPG of 8 mmHg. The median PLT was 10.8 G/L and the median LSM was 15.3 kPa, respectively. Diagnostic performance of the SHAPE methodology in this population for CSPH was also noteworthy, demonstrating a PPV of 89% and a NPV of 89% (AUC: 0.90).

Discussion

To our best knowledge, this is the first study to comprehensively benchmark the revised SHAPE method against multiple established non-invasive CSPH models, including Baveno VII and Baveno VII-SSM criteria[5,8]. In contrast to previous research that primarily examined correlation strength[18], our study is the first to directly benchmark the classification accuracy of SHAPE against multiple validated CSPH models, establishing its diagnostic superiority. Our findings confirm its superior diagnostic accuracy and ability to eliminate indeterminate cases, addressing a key limitation of current non-invasive approaches.

The present study demonstrates that the revised SHAPE method is a robust and clinically useful non-invasive approach for evaluating CSPH. The SHAPE gradient exhibited an exceptionally strong correlation with HVPG and demonstrated significantly higher diagnostic accuracy than the Baveno VII and Baveno VII-SSM criteria. Additionally, the SHAPE methodology surpassed established serum markers of fibrosis and prognosis, reinforcing its potential as a primary non-invasive screening tool. Importantly, SHAPE substantially reduced the proportion of patients in the diagnostic gray zone, highlighting its potential clinical applicability.

Th current study introduces several novel contributions to the field. First, we optimized the SHAPE acquisition by standardizing the protocol, integrating a bolus injection method, and employing commercial software, enhancing clinical feasibility and reproducibility. The use of perfluorobutane-based contrast agents demonstrated excellent interobserver agreement. This choice not only ensured high reproducibility but also aligns with widely available ultrasound contrast protocols, making SHAPE adaptable across diverse clinical

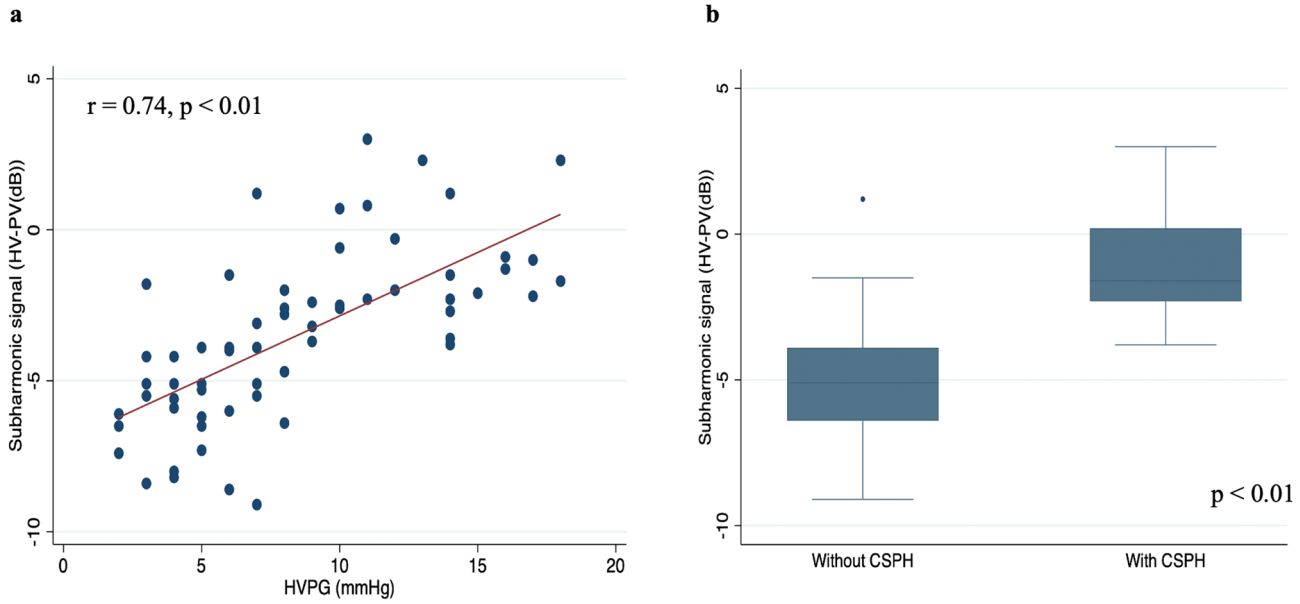

Fig. 3. Scatterplot showing the correlation between the SHAPE gradient (HV-PV) and HVPG (**a**). Box plot showing the SHAPE gradient (HV-PV) in patients without CSPH (HVPG < 10 mmHg) and in those with CSPH (HVPG ≥ 10 mmHg) (**b**). CSPH, clinically significant portal hypertension; HV, hepatic vein; HVPG, hepatic venous pressure gradient; PV, portal vein; SHAPE, subharmonic-aided pressure estimation.

settings. Second, unlike previous studies that mainly reported correlations with HVPG[18], we directly compared SHAPE against established diagnostic algorithms and quantified its ability to resolve indeterminate cases. Lastly, our cohort included patients with diverse liver disease etiologies, including metabolic dysfunction-associated liver disease and alcohol-associated liver disease, providing insights relevant to real-world clinical populations.

Previous studies, including those by Machado et al. and Kuroda et al., explored the utility of contrast-enhanced ultrasonography in assessing PH[14,17]. Gupta et al. reported a strong correlation (r = 0.68) between the SHAPE gradient and HVPG[18]. Our study demonstrated an even stronger correlation, supporting the refinement and reliability of our technique. Moreover, we improved clinical feasibility by employing a bolus injection protocol and commercial software.

While the LSM remains a widely validated tool for CSPH assessment[1,20], approximately half of patients remain in the diagnostic gray zone under Baveno VII criteria[21]. Incorporating SSM improves diagnostic accuracy[8,22] but has technical limitations. In our study, the revised SHAPE method outperformed all three Baveno VII-based models in terms of sensitivity, specificity, and the complete elimination of the gray zone.

The present study has limitations. It was a retrospective, single-center analysis with a small sample size; external validity was limited, however, this sample size was strategically designed on the basis of power calculations, ensuring sufficient statistical strength to detect meaningful correlations between SHAPE and HVPG. Despite its modest scope, the observed strong performance metrics validate its robustness. The study was designed as a proof-of-concept diagnostic validation and provides a strong foundation for future multicenter trials. Additionally, contrast-enhanced ultrasonography is operator-dependent and SHAPE requires technical expertise Further, the cost of contrast agent must be considered. Broader applicability will depend on equipment availability and operator training. Finally, the influence of selection bias in our study cannot be ignored and may affect the interpretation of our findings. Future research should explore interobserver consistency in larger populations with multicenter validation, evaluate prognostic value, and assess performance across various etiologies.

In conclusion, the refined SHAPE method offers a standardized, practical, and highly accurate approach to CSPH diagnosis, overcoming the limitations of existing models. By eliminating indeterminate cases and achieving superior diagnostic accuracy, SHAPE represents a remarkable advancement in non-invasive PH assessment. Future research should expand SHAPE validation to multicenter trials and assess its prognostic value in CSPH progression and treatment response. Given its remarkable diagnostic accuracy, SHAPE holds promise as an indispensable component of routine clinical assessment.

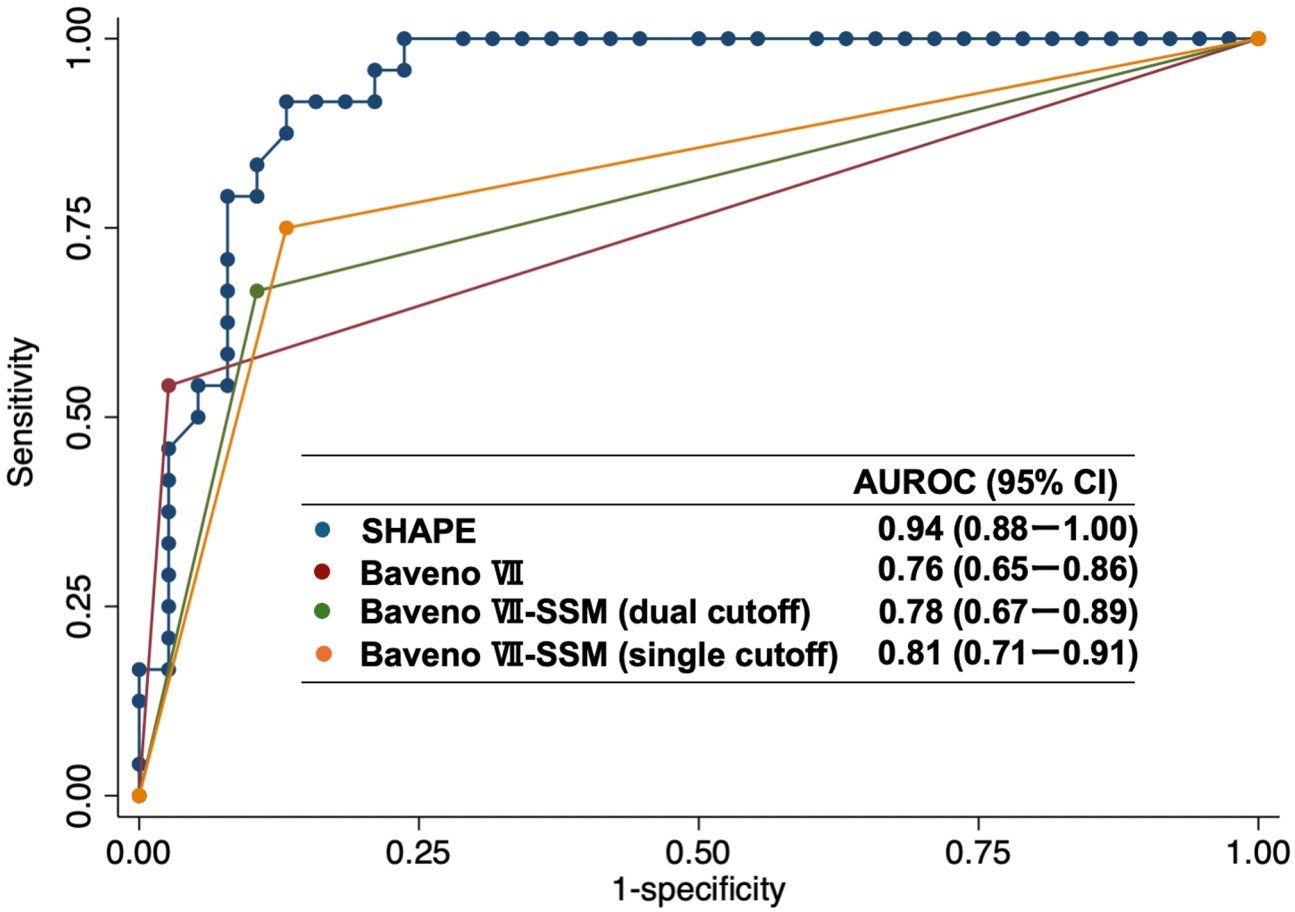

Fig. 4. ROC curve analysis for discriminating patients with CSPH. The AUC values are 0.94, 0.76, 0.78, and 0.81 for the SHAPE gradient (HV-PV), Baveno VII criteria, Baveno VII-SSM dual cutoff, and Baveno VII-SSM single cutoff models, respectively. ROC, receiver operating characteristic; AUC, area under the receiver operating characteristic; CSPH, clinically significant portal hypertension; HV, hepatic vein; PV, portal vein; SHAPE, subharmonic-aided pressure estimation.

	SHAPE gradient	Baveno VII	Baveno VII-SSM (dual cutoff)	Baveno VII-SSM (single cutoff)
AUC (95% CI)	0.94 (0.88–1.00)	0.76 (0.65–0.86)	0.78 (0.67–0.89)	0.81 (0.71–0.91)
Ruled-in cutoff value	− 2.7 (dB)	LSM ≥ 25 kPa	Two out of the following: LSM ≥ 25 kPa, PLT < 150 G/L, and/or SSM > 50 kPa	Two out of the following: LSM ≥ 25 kPa, PLT < 150 G/L, and/or SSM > 40 kPa
Ruled-out cutoff value		LSM ≤ 15 kPa and PLT ≥ 150 G/L	Two out of the following: LSM ≤ 15 kPa, PLT ≥ 150 G/L, and/or SSM < 21 kPa	Two out of the following: LSM ≤ 15 kPa, PLT ≥ 150 G/L, and/or SSM ≤ 40 kPa
Sensitivity	0.92	0.54	0.67	0.75
Specificity	0.87	0.97	0.89	0.87
PPV	0.81	0.93	0.84	0.82
NPV	0.94	0.95	0.96	0.94
LR +	6.97	20.5	6.33	5.70
LR-	0.09	0.47	0.37	0.29
Gray zone, n (%)		27 (44)	17 (27)	9 (15)

Table 2. Diagnostic performance of the SHAPE gradient, Baveno VII criteria alone and as part of algorithms for patients with CSPH. *AUC* area under the receiver-operator curve; *CI* confidence interval; *CSPH* clinically significant portal hypertension; *LR* + positive likelihood ratio; *LR* negative likelihood ratio; *LSM* liver stiffness measurement; *NPV* negative predictive value; *PLT* platelet count; *PPV* positive predictive value; *SSM* spleen stiffne.

Data availability

The datasets generated and/or analyzed during the current study are available from the corresponding author on reasonable request.

Received: 25 June 2025; Accepted: 27 October 2025
Published online: 26 November 2025

References

1. Garcia-Tsao, G., Abraldes, J. G., Berzigotti, A. & Bosch, J. Portal hypertensive bleeding in cirrhosis: Risk stratification, diagnosis, and management: 2016 practice guidance by the American association for the study of liver diseases. *Hepatology* **65**, 310–335 (2017).
2. Imai, Y. et al. Standard technique in Japan for measuring hepatic venous pressure gradient. *J. Gastroenterol.* **60**, 24–31 (2025).
3. Vuille-Lessard, É., Rodrigues, S. G. & Berzigotti, A. Noninvasive detection of clinically significant portal hypertension in compensated advanced chronic liver disease. *Clin. Liver Dis.* **25**, 253–289 (2021).
4. Berzigotti, A., Ashkenazi, E., Reverter, E., Abraldes, J. G. & Bosch, J. Non-invasive diagnostic and prognostic evaluation of liver cirrhosis and portal hypertension. *Dis. Markers* **31**, 129–138 (2011).
5. de Franchis, R. et al. Baveno VII—Renewing consensus in portal hypertension. *J. Hepatol.* **76**, 959–974 (2022).
6. Kaplan, D. E. et al. AASLD practice guidance on risk stratification and management of portal hypertension and varices in cirrhosis. *Hepatology* **79**, 1180–1211 (2024).
7. Sterling, R. K. et al. AASLD practice guideline on noninvasive liver disease assessment of portal hypertension. *Hepatology* **81**, 1060–1085 (2025).
8. Dajti, E. et al. Accuracy of spleen stiffness measurement for the diagnosis of clinically significant portal hypertension in patients with compensated advanced chronic liver disease: A systematic review and individual patient data meta-analysis. *Lancet Gastroenterol. Hepatol.* **8**, 816–828 (2023).
9. Frinking, P. J., Brochot, J. & Arditi, M. Subharmonic scattering of phospholipid-shell microbubbles at low acoustic pressure amplitudes. *IEEE Trans. Ultrason. Ferroelectr. Freq. Control* **57**, 1762–1771 (2010).
10. Gupta, I. et al. Effect of pulse shaping on subharmonic aided pressure estimation *in vitro* and *in vivo*. *J. Ultrasound Med.* **36**, 3–11 (2017).
11. Dave, J. K. et al. Non-invasive intra-cardiac pressure measurements using subharmonic-aided pressure estimation: Proof of concept in humans. *Ultrasound Med. Biol.* **43**, 2718–2724 (2017).
12. Halldorsdottir, V. G. et al. Subharmonic contrast microbubble signals for noninvasive pressure estimation under static and dynamic flow conditions. *Ultrason. Imaging* **33**, 153–164 (2011).
13. Mayer, H. et al. Investigation into the subharmonic response of three contrast agents in static and dynamic flow environments using a commercially available diagnostic ultrasound scanner. *Ultrasound Med. Biol.* **50**, 1731–1738 (2024).
14. Kuroda, H. et al. Novel subharmonic-aided pressure estimation for identifying high-risk esophagogastric varices. *J. Gastroenterol.* **60**, 187–196 (2025).
15. Eisenbrey, J. R. et al. Simultaneous grayscale and subharmonic ultrasound imaging on a modified commercial scanner. *Ultrasonics* **51**, 890–897 (2011).
16. Eisenbrey, J. R. et al. Chronic liver disease: Noninvasive subharmonic aided pressure estimation of hepatic venous pressure gradient 1. *Radiology* **268**, 581–588 (2013).
17. Machado, P. et al. Hepatic vein contrast-enhanced ultrasound subharmonic imaging signal as a screening test for portal hypertension. *Dig. Dis. Sci.* **66**, 4354–4360 (2021).
18. Gupta, I. et al. Diagnosing portal hypertension with noninvasive subharmonic pressure estimates from a US contrast agent. *Radiology* **298**, 104–111 (2021).
19. Halldorsdottir, V. G. et al. Subharmonic-aided pressure estimation for monitoring interstitial fluid pressure in tumors: Calibration and treatment with paclitaxel in breast cancer xenografts. *Ultrasound Med. Biol.* **43**, 1401–1410 (2017).
20. You, M. W. et al. A meta-analysis for the diagnostic performance of transient elastography for clinically significant portal hypertension. *Ultrasound Med. Biol.* **43**, 59–68 (2017).
21. Jachs, M. et al. The sequential application of Baveno VII criteria and vitro score improves diagnosis of clinically significant portal hypertension. *Clin. Gastroenterol. Hepatol.* **21**, 1854-1863.e10 (2023).
22. Hirooka, M. et al. Accurate reflection of hepatic venous pressure gradient by spleen stiffness measurement in patients with low controlled attenuation parameter values. *JGH Open* **5**, 1172–1178 (2021).

Author contributions

Study concept and design: MH and YH. Acquisition of data: YN, MH, RY, NF, TS, MM, YO, AY, TW, OY, YT and MA. Analysis and interpretation of data: YN, MH and RY. Manuscript drafting: YN. Critical revision of the manuscript for important intellectual content: NK, TO and MH. Statistical analysis: HK and MF. Obtained funding: MH and YH. Administrative, technical, or material support: NK and TO. Study supervision: YH.

Funding

This work was supported in part by the Japan Society for the Promotion of Science KAKENHI (grant number: 21K07701 to M.H. and grant number: 21K08008 to Y.H.).

Declarations

Conflict of interest

The authors declare that they have no conflict of interest.

Consent to participate

The requirement for informed consent was waived because of the retrospective study design.

Ethical approval

Approval of the research protocol: This study was approved by the Institutional Ethics Committee of Ehime University Hospital (approval number: 2410005, date of approval: October 23, 2024) and was conducted in

agreement with the principles of the Declaration of Helsinki.

Additional information

Supplementary Information The online version contains supplementary material available at https://doi.org/10.1038/s41598-025-26100-2.

Correspondence and requests for materials should be addressed to M.H.

Reprints and permissions information is available at www.nature.com/reprints.

Publisher's note Springer Nature remains neutral with regard to jurisdictional claims in published maps and institutional affiliations.